European Journal of Medicinal Chemistry 50 (2012) 405–415

Contents lists available at SciVerse ScienceDirect

European Journal of Medicinal Chemistry

journal homepage: http://www.elsevier.com/locate/ejmech

Original article

Evaluation of DNA binding, antioxidant and cytotoxic activity of mononuclear Co(III) complexes of 2-oxo-1,2-dihydrobenzo[h]quinoline-3-carbaldehyde thiosemicarbazones

Eswaran Ramachandran [a], Sajesh P. Thomas [b], Paramasivan Poornima [c], Palaniappan Kalaivani [a], Rathinasabapathi Prabhakaran [a], Viswanadha Vijaya Padma [c], Karuppannan Natarajan [a,*]

[a] Department of Chemistry, Bharathiar University, Coimbatore 641046, India
[b] Solid State and Structural Chemistry Unit, Indian Institute of Science, Bangalore 560 012, India
[c] Department of Biotechnology, Bharathiar University, Coimbatore 641 046, India

ARTICLE INFO

Article history:
Received 20 January 2012
Received in revised form
10 February 2012
Accepted 13 February 2012
Available online 18 February 2012

Keywords:
Cobalt(III) complexes
Benzo[*h*]quinoline
Thiosemicarbazones
DNA binding
Antioxidant

ABSTRACT

Four new 2-oxo-1,2-dihydrobenzo[*h*]quinoline-3-carbaldehyde N-substituted thiosemicarbazone ligands (H_2-LR, where R = H, Me, Et or Ph) and their corresponding new cobalt(III) complexes have been synthesized and characterized. The structures of the complexes **2** and **3** were determined by single crystal X-ray diffraction analysis. The interactions of the new complexes with DNA were investigated by absorption, emission and viscosity studies which indicated that the complexes bind to DNA via intercalation. Antioxidant studies of the new complexes showed that the significant antioxidant activity against DPPH radical. In addition, the *in vitro* cytotoxicity of complexes **1**–**4** against A549 cell line was assayed which showed higher cytotoxic activity with lower IC_{50} values indicating their efficiency in killing the cancer cells even at very low concentrations.

1. Introduction

Cancer is one of the fatal diseases, which claims over 6 million people each year worldwide and is still increasing. The majority of drugs used for the treatment of cancer today are not 'cancer cell-specific' and potently cytotoxic against normal cells. So, the most rapidly developing area of pharmaceutical research is the discovery of new drugs for cancer therapy. In this regard, cisplatin is widely used and well-known metal-based drug for cancer therapy, but it possesses inherent limitations such as side effects and low administration dosage [1–4]. Therefore, attempts are being made to replace this drug with suitable alternatives, and numerous transition-metal complexes have been synthesized and screened for their anticancer activities. Metals, in particular transition metals offer potential advantages over the more common organic-based drugs, including a wide range of coordination numbers and geometries, accessible redox states, 'tune-ability' of the thermodynamics and kinetics of ligand substitution, and a wide structural diversity. Among the transition metals, cobalt is an element of biological interest and its role is mainly focused on its presence in the active centre of vitamin B12, which regulates indirectly the synthesis of DNA [5]. In addition, among the metal complexes that have been studied, cobalt complex containing nitrogen heterocyclic thiosemicarbazone is of interest because of its biological activities and ability to bind to DNA [6–10]. In the case of pharmaceuticals, in addition to thiosemicarbazones, nitrogen heterocycles have also exhibited remarkable biological activities [11–13]. In particular, some derivatives of 2-oxoquinoline have shown biological activities such as antioxidation, antiproliferation, anti-inflammation, and anticancer [14–17]. We have recently reported the reactions of thiosemicarbazones and heterocycles of thiosemicarbazones with transition metal ions in an attempt to examine their mode of binding and possible biological relevance of the resulting complexes [18–20]. In addition, we have also reported the effect of substitution on terminal N of thiosemicarbazones on the biological properties of the complexes formed [21,22]. Though an extensive amount of work has been done on various thiosemicarbazones, no work seems to have been done on thiosemicarbazones prepared from 2-oxo-1,2-dihydro-benzo[h]quinoline-3-carbaldehyde. This aroused our interest in the syntheses of 2-oxo-1,2-dihydro-benzo

* Corresponding author. Tel.: +91 422 2428319; fax: +91 422 2422387.
E-mail address: k_natraj6@yahoo.com (K. Natarajan).

0223-5234/$ – see front matter © 2012 Elsevier Masson SAS. All rights reserved.
doi:10.1016/j.ejmech.2012.02.026

[h]quinoline-3-carbaldehyde thiosemicarbazones, and their cobalt(III) complexes with a viewpoint towards evaluating their effect of substitution on terminal nitrogen of thiosemicarbazones on biological properties such as DNA binding, antioxidative and cytotoxic activity.

Herein, we report the synthesis, characterization, DNA binding, antioxidative and cytotoxicity studies of new cobalt(III) complexes of 2-oxo-1,2-dihydro-benzo[h]quinoline-3-carbaldehyde N-substituted thiosemicarbazones. The crystal structures of **2** and **3** have been determined by X-ray crystallography. The investigation of the biological properties of the cobalt(III) complexes has been focused on the binding properties with calf thymus (CT-DNA) performed by UV spectroscopy, DNA solution viscosity measurements, and competitive binding studies with ethidium bromide (EB).

2. Results and discussion

2.1. Synthesis and characterization

The synthetic routes for the ligands and its corresponding cobalt(III) complexes are shown in Scheme 1. The ligands (H_2L1), (H_2L2), (H_2L3) and (H_2L4) were prepared by the condensation reaction of 2-oxo-1,2-dihydro-benzo[h]quinoline-3-carbaldehyde with corresponding 4-N-substituted thiosemicarbazide in methanol medium. They were characterized by elemental analysis, IR spectroscopy and ^{1}H NMR spectroscopy. The assignments for the IR and ^{1}H NMR spectra are given in the Experimental section. The new cobalt(III) complexes were prepared by the direct reaction of the appropriate ligand with $Co(NO_3)\cdot 6H_2O$ in methanol medium in good yields. The single crystals of new cobalt(III) complexes (**2** and **3**) were isolated by slow evaporation of the reaction mixture over a period of few days. The IR peak shift in ν(C=O) and ν(C=N) and the peak disappearance of ν(C=S) of the ligand in the complex gave evidence for coordination of the ligands to cobalt ion in the complexes. The ^{1}H-NMR spectra of the new cobalt complexes when compared with those of free ligands, did not show the signal for N(3)H indicating that ligand coordinated to the Co(III) ion in all the complexes in the thiolate form. These observations have also been confirmed by X-ray single crystal structure analysis.

The electronic spectra of the free ligands exhibit bands at 291 nm and 335 nm corresponding to the n → π* transition of the imine portion and π → π* transitions of the aromatic ring, respectively. The intense absorption bands observed for all the complexes in the regions of 279–282 and 431–441, 455–463 nm are attributed to the intra ligand π → π* transitions within the coordinated ligand moiety and imines and ligand-to-metal charge-transfer (LMCT) transitions respectively. The single crystal X-ray analysis showed that formula of the complexes are $[Co(HL)_2]NO_3\cdot 4H_2O$. Table 1 summarizes the crystal data, data collection and refinement parameters for the new Co(III) complexes.

2.2. Crystal structure of the complexes *2* and *3*

The ORTEP diagram of the complex **2** and **3** including the atom numbering scheme are shown in Figs. 1 and 2, respectively and the selected bond lengths and bond angles are listed in Table 2. X-ray crystallographic data of all complexes revealed that mononuclear cation complexes neutralized by one nitrate anion. The coordination geometry around Co(III) cation can be described as a distorted octahedron, the cobalt atom being bonded to two tridentate ONS donor ligand molecules in such a way that two five member and two six member chelate rings are formed. And in complexes **2** and **3** the two oxygen, two nitrogen and two sulphur atoms exhibit ligand-metal-ligand bite angles are found to be S1–Co1–N2 85.1(3)°; S2–Co1–N6, 85.8(3)°; O1–Co1–N2, 94.5(3)°; O2–Co1–N6, 94.0(3)° and S1–Co1–N2, 86.88(15)°; S2–Co1–N6, 86.35(12)°; O1–Co1–N2, 94.41(18)°; O2–Co1–N6, 93.74(16)° respectively. The *trans* angles of the complex **2** and **3** [O1–Co1–S1, 177.0 (2)°, O2–Co1–S2, 178.5(2)°; N2–Co1–N6, 175.6(4)° and O1–Co1–S1, 177.25(11)° O2–Co1–S2, 176.91(13)°; N2–Co1–N6, 177.81(18)° respectively] deviate slightly from the expected linear trans geometry. In complex **2**, two crystallograhically independent molecules present in the asymmetric unit. The C–S bond distance increased from the reported value of C=S 1.6750(14) Å in the free ligand to 1.738(3) Å [S(2)–C(6)] and 1.743(2) Å [S(4)–C(12)] in the cobalt complexes [23]. Likewise, there was a diminution of the carbon-hydrazinic nitrogen bond length from 1.365(3) Å [N(3)–C(6)] in the free ligands to 1.339(3) Å [N(3)–C(6)] and 1.325(3) Å [N(7)–C(12)] in the complexes. These facts indicate that the ligand is deprotonated and shifts from the thione to the thiolate form, in such a way that the negative charge is delocalized between the two bonds [24].

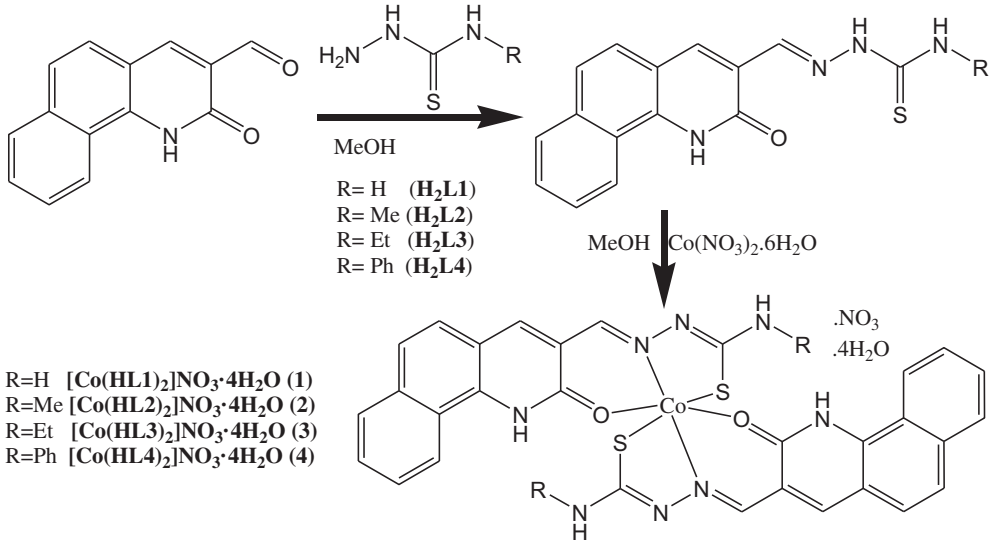

Scheme 1. Preparation of the ligands and it corresponding cobalt(III) complexes.

Table 1
Experimental data for crystallographic analyses.

	Complex **2**	Complex **3**
CCDC number	861,100	861,101
Empirical formula	$C_{32}H_{34}CoN_9O_9S_2$	$C_{34}H_{34}CoN_9O_9S_2$
Formula weight	809.74	831.79
Temperature/K	100(2)	100(2)
Crystal system	Triclinic	Monoclinic
Space group	*P*−1	*C*2/*c*
a(Å)	14.8718(16)	19.1566(17)
b(Å)	16.1264(17)	29.8145(19)
c(Å)	17.647(3)	15.1055(13)
α(°)	112.450(11)	90.00
β(°)	104.033(11)	120.731(12)
γ(°)	103.809(9)	90.00
Volume/Å^3	3526.2(7)	7415.9(10)
Z	4	8
ρ_{calc}mg/mm^3	1.841	1.490
m/mm^{-1}	1.890	0.642
F(000)	1988	3424
Crystal size/mm^3	0.25 × 0.20 × 0.20	0.20 × 0.20 × 0.20
Theta range for data collection	2.4–26.0°	2.4–25.0°
Index ranges	$-18 \le h \le 18$ $-19 \le k \le 19$ $-21 \le l \le 21$	$-22 \le h \le 22$ $-35 \le k \le 35$ $-17 \le l \le 17$
Reflections collected	29,812	35,969
Independent reflections	13,832[R(int) = 0.1281]	6531[R(int) = 0.1325]
Data/restraints/parameters	13,832/18/995	6531/0/502
Goodness-of-fit on F^2	1.015	1.116
Final R indexes [I > 2σ (I)]	$R_1 = 0.1528$, $wR_2 = 0.3534$	$R_1 = 0.0857$, $wR_2 = 0.2206$
Final R indexes [all data]	$R_1 = 0.2645$, $wR_2 = 0.4188$	$R_1 = 0.1360$, $wR_2 = 0.2640$
Largest diff. peak/hole/e Å^{-3}	2.349/−0.800	1.29/−0.67

The dihedral angle between the mean planes of the five-member chelation ring and the six member one is 11.92°, 10.22° and 13.03°, 6.57°for **2** and **3** respectively. The crystal packing in **2** and **3** is stabilized by O–H···O and N–H···O hydrogen bonds. In complex **2,** these hydrogen bonds are facilitated by the amino nitrogen atom N(4) and aromatic nitrogen atom N(1) which act as hydrogen bond donors and N(3) acting as acceptor. In complex **3,** aromatic nitrogen N(1) acts as hydrogen bond donor and 2-oxo oxygen atom acts as acceptor. Further, solvent water molecules play an important role in stabilizing the supra molecular assemblies in the crystal structures of **2** and **3.**

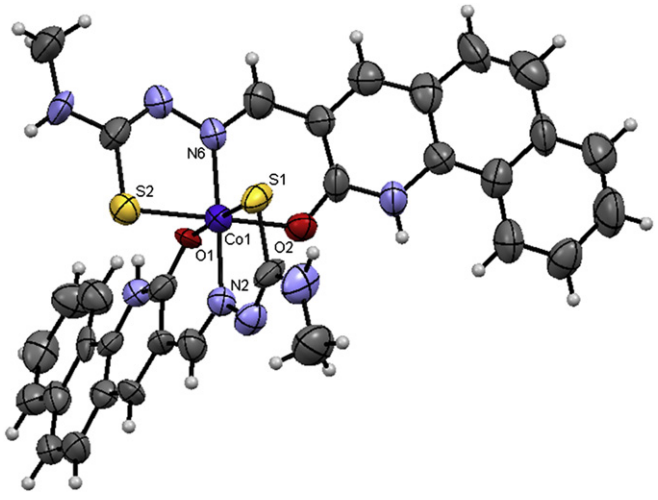

Fig. 1. ORTEP views of Complex **2**. The nitrate ion and water molecules have been omitted for clarity.

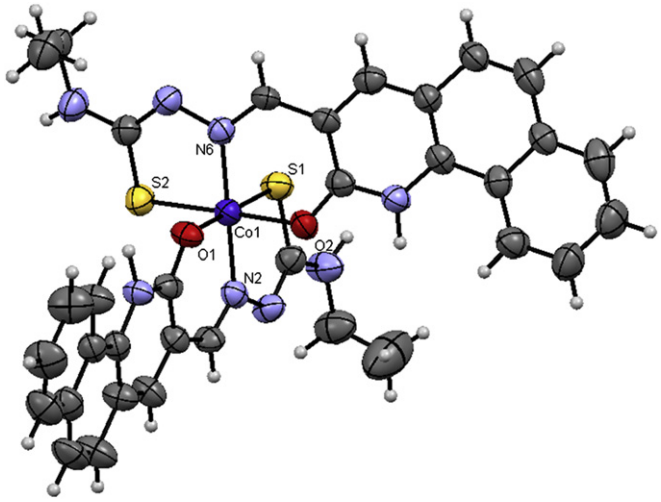

Fig. 2. ORTEP views of Complex **3**. The nitrate ion and water molecules have been omitted for clarity.

Based on the analytical, spectroscopic characterization (FT–IR, UV–visible and NMR) and single-crystal X-ray crystallographic studies for complexes **2** and **3**, the octahedral structure has been proposed for all the new Co(III) complexes (Scheme 1).

2.3. DNA binding studies

It is a well-known fact that DNA binding studies is the preliminary pharmacological target of many antitumor compounds, and hence, the interaction between DNA and metal complex is of paramount importance in understanding the mechanism. Thus, the mode and tendency for binding of complexes **1**–**4** to CT-DNA were studied with the aid of different techniques.

2.3.1. Electronic absorption titration

Of all the techniques used, electronic absorption spectroscopy is one of the most common techniques for the investigation of the mode of interaction of metal complexes with DNA [25,26]. A compound binding to DNA through intercalation usually results in

Table 2
Selected bond lengths (Å) and bond angles (°) for the complexes **2** and **3**.

	Complex **2**	Complex **3**
Co1–S1	2.228(3)	2.1934(17)
Co1– S2	2.201(3)	2.2028(15)
Co1–O1	2.024(8)	1.964(4)
Co1– O2	1.954(7)	1.960(3)
Co1–N6	1.904(9)	1.902(4)
Co1– N2	1.903(9)	1.918(4)
O1–Co1–S1	177.03(2)	177.25(11)
O1–Co1–S2	92.3(2)	89.79(11)
O2–Co1–S1	90.9(2)	90.50(12)
O2–Co1–S2	178.5(2)	176.91(13)
O2–Co1–O1	86.2(3)	87.13(16)
N2–Co1–S1	85.1(3)	86.88(15)
N2–Co1–S2	91.0(3)	92.47(13)
N2–Co1–O1	94.5(3)	94.41(18)
N2–Co1–O2	89.2(3)	87.54(16)
N6–Co1–S1	91.9(3)	91.34(14)
N6–Co1–S2	85.8(3)	86.35(12)
N6–Co1–O1	88.8(3)	87.43(17)
N6–Co1–O2	94.0(3)	93.74(16)
N6–Co1–N2	175.6(4)	177.81(18)
S1–Co1–S2	90.62(12)	92.59(6)

hypochromism with or without a small red or blue shift, due to the intercalative mode involving a strong stacking interaction between the planar aromatic chromophore and the base pairs of DNA [27,28]. The absorption spectra of complexes in the absence and presence of CT-DNA are given in Fig. 3. Upon increasing the concentration of DNA, the absorption band of complex **1** at 309, 440 and 463 nm exhibit hypochromism of 38.17%, 27.18% and 25.52%, with red shift of 5, 3, and 5 nm respectively, whereas the absorption bands of complex **2** at 309 and 463 nm, exhibits hypochromism of 74.50% and 66.79%, with red shift of 11 and 6 nm, respectively. Complex **3** at 279, 447 and 463 nm, and complex **4** at 300, 437 and 458 nm exhibited a hypochromism of about 75.30, 56.29%, and 54.80% and 76.45%, 62.17% and 61.38% with a red shift of 32, 4 and 9 nm and 6, 3 and 5 nm respectively. These results suggested that complexes **1**–**4** are likely to bind to the DNA helix via intercalation, due to stacking interaction between the planar aromatic chromophore and the base pairs of DNA. The complex **4** showed more hypochromicity than the remaining complexes, indicating that the binding strength of the complex **4** is much stronger than the other three complexes. In order to compare the binding strength of the complexes, their intrinsic binding constants (K_b) can be determined from the following equation [29].

$$[DNA]/(\varepsilon_a - \varepsilon_f) = [DNA]/(\varepsilon_b - \varepsilon_f) + 1/K_b(\varepsilon_b - \varepsilon_f)$$

where, [DNA] is the concentration of DNA in the base pairs, ε_a is the apparent absorption coefficient corresponding to A_{obs}/[compound], ε_f is the extinction coefficient of the free compound and ε_b is the extinction coefficient of the compound when fully bound to DNA. From the plot of [DNA]/($\varepsilon_a - \varepsilon_f$) versus [DNA] (Fig. 4), K_b is calculated from the ratio of the slope to the intercept. The intrinsic binding constant (K_b) values were 2.90(±0.09) × 10^4 M^{-1}, 6.03(±0.05) × 10^4 M^{-1}, 6.16(±0.05) × 10^4 M^{-1} and 8.79(±0.03) × 10^4 M^{-1} for complexes **1**, **2**, **3** and **4** respectively. The observed values of K_b revealed that new cobalt complexes bind to DNA via the intercalative mode. From the results obtained, it has been found that complex **4** strongly bind with CT-DNA compared to other complexes and the order of binding affinity is **1** < **2** ≈ **3** < **4**. From the electronic absorption studies, though it has been found that the four complexes can bind to DNA by intercalation, the binding mode need to be proved through some more experiments.

2.3.2. Fluorescence spectral studies

The emission experiment has been widely used to further confirm the interaction between the test complexes and CT-DNA. The results of fluorescence titration spectra have also been confirmed to be effective for characterizing the binding mode of the metal complexes to DNA. Since all the four new complexes emitted weak luminescence in the phosphate buffered saline at room temperature, fluorescence spectral studies were carried out. Fig. 5 shows the results of the emission titration curve of the complexes with CT-DNA. An increase in DNA concentration resulted an increase in the emission intensity of the Co(III) complexes. Upon increasing the concentration of CT-DNA, the emission intensity of complexes **1**–**4** at 526, 525, 526 and 523 nm increased by around 1.33, 1.49, 1.59 and 1.62 times, respectively, in comparison to the same in the absence of DNA. This phenomenon is related

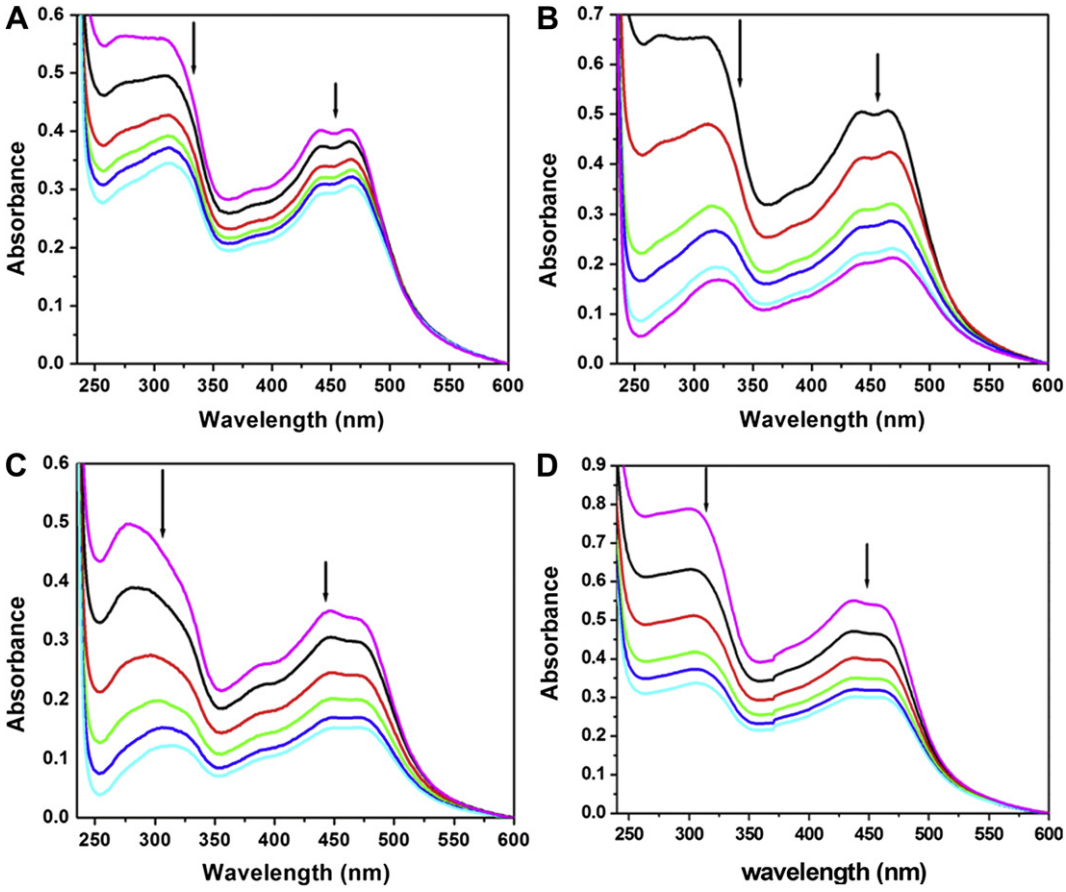

Fig. 3. Electronic spectra of the complex **1**(A), **2**(B), **3**(C) and **4**(D) in Tris–HCl buffer upon addition of CT-DNA. [Compound] = 25 μM, [DNA] = 0–25 μM. Arrow shows the absorption intensities decrease upon increasing DNA concentration.

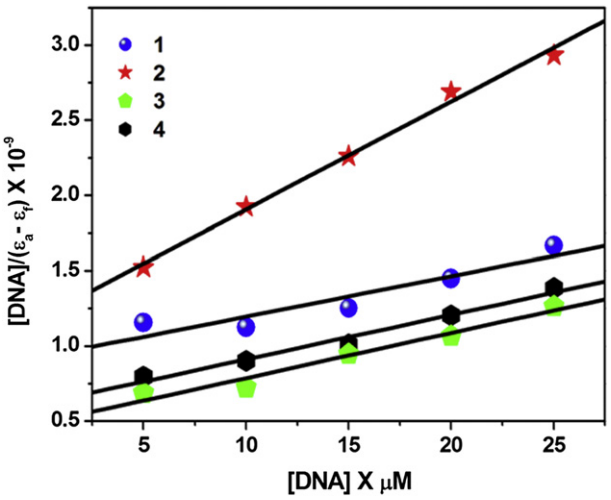

Fig. 4. Plots of $[DNA]/(\varepsilon_a - \varepsilon_f)$ versus [DNA] for the complexes **1**–**4** with CT-DNA.

to the extent to which the compound penetrates into the hydrophobic environment inside the DNA, thereby avoiding the quenching effect of solvent water molecules. The binding of complexes to CT-DNA leads to a marked increase in the emission intensity, which also agrees with those observed for other intercalators [27,28,30]. These results revealed that the complexes bind to DNA via intercalation mode.

2.3.3. Ethidium bromide (EB) displacement studies

The absorption titration results indicate that the complexes effectively bind to DNA. In order to confirm the binding mode and compare their binding affinities, ethidium bromide displacement experiments were carried out. EB is a planar cationic dye which is widely used as a sensitive fluorescence probe for native DNA. EB emits intense fluorescent light in the presence of DNA due to its strong intercalation between the adjacent DNA base pairs [31,32]. Hence, EB displacement technique can provide indirect evidence for the DNA binding mode. The displacement technique is based on the decrease of fluorescence resulting from the displacement of EB from a DNA sequence by a quencher and the quenching is due to the reduction of the number of binding sites on the DNA that is available to the EB. Fig. 6 shows the fluorescence quenching spectra of DNA-bound EB by complexes and illustrate that as the concentration of the complexes increases, the emission band at 603 nm exhibited hypochromism up to 55.86, 60.72, 64.53 and 70.05% of the initial fluorescence intensity for **1**, **2**, **3** and **4** respectively. The observed decrease in the fluorescence intensity clearly indicates that the EB molecules are displaced from their DNA binding sites and are replaced by the compounds under investigation [33]. The quenching parameter can be analyzed according to the Stern–Volmer equation,

$$F^0/F = K_q[Q] + 1$$

where F^0 is the emission intensity in the absence of compound, F is the emission intensity in the presence of compound, K_q is the quenching constant, and [Q] is the concentration of the compound.

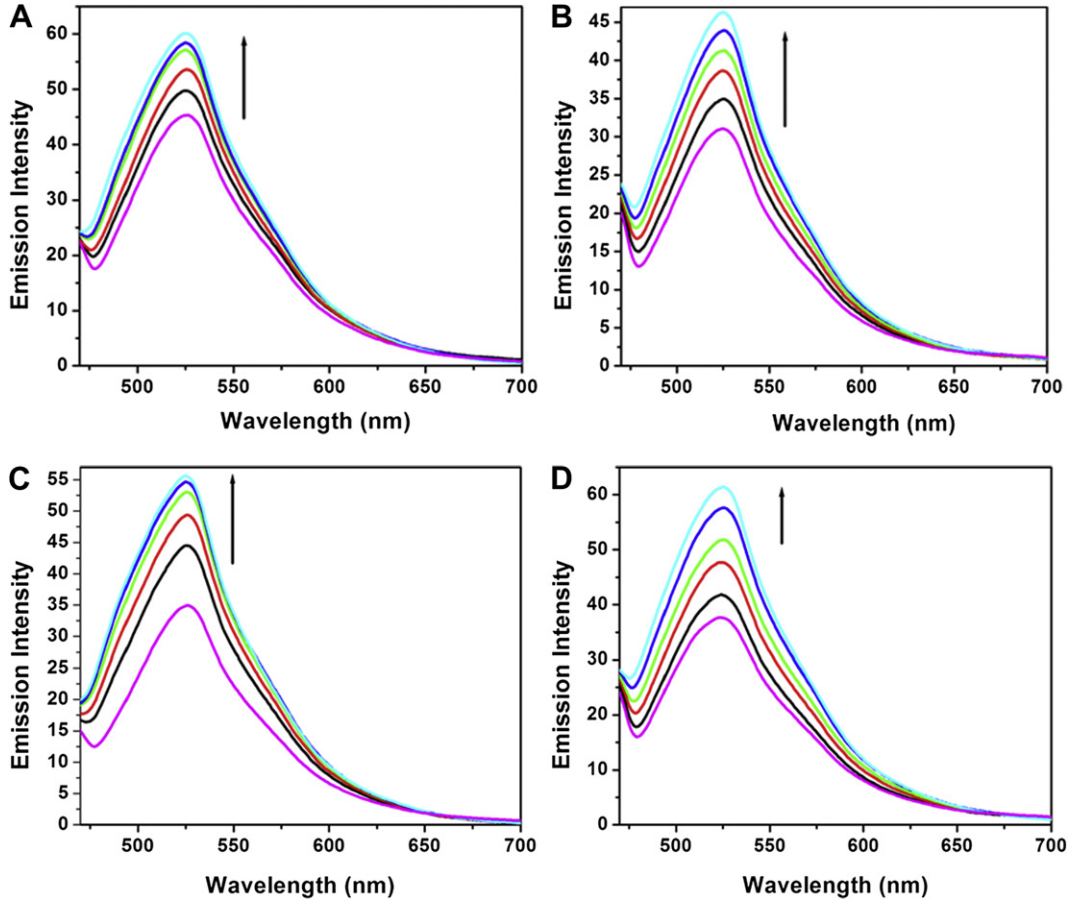

Fig. 5. Emission enhancement spectra of complexes **1**(A), **2**(B), **3**(C) and **4**(D) (25 μM) in the presence of increasing amounts of CT-DNA (0–25 μM; subsequent spectra). The arrow shows the emission intensity increases upon increasing the DNA concentration.

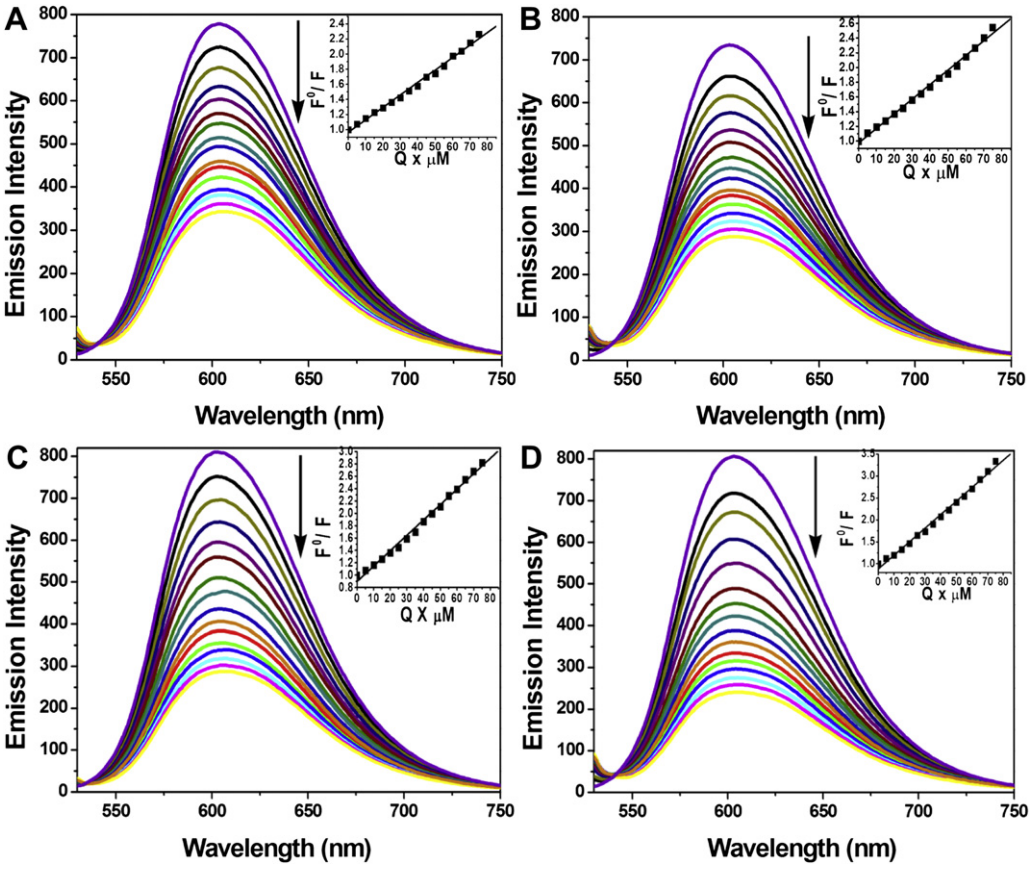

Fig. 6. Fluorescence quenching curves of ethidium bromide bound to DNA: **1**(A), **2**(B), **3**(C) and **4**(D). [DNA] = 12 μM, [EB] = 12 μM, and [compound] = 0–75 μM. Inset: Stern–Volmer plots of the fluorescence titrations of **1**, **2**, **3** and **4**.

The K_q value is obtained as a slope from the plot of F^0/F versus [Q]. In the Stern–Volmer plot (inset in Fig. 6) of F^0/F versus [Q], the quenching constant (K_q) is obtained from the slope which was $1.65 \times 10^4\ M^{-1}$, $1.99 \times 10^4\ M^{-1}$, $2.49 \times 10^4\ M^{-1}$ and $3.10 \times 10^4\ M^{-1}$ for the complexes **1, 2, 3** and **4** respectively. Further, the apparent DNA binding constant (K_{app}) were calculated using the following equation,

$$K_{EB}[EB] = K_{app}[complex]$$

(where the compound concentration is the value at a 50% reduction in the fluorescence intensity of EB, K_{EB} ($1.0 \times 10^7\ M^{-1}$) is the DNA binding constant of EB, [EB] is the concentration of EB = 12 μM), and it was found to be $1.98 \times 10^6\ M^{-1}$, $2.38 \times 10^6\ M^{-1}$, $2.99 \times 10^6\ M^{-1}$ and $3.72 \times 10^6\ M^{-1}$ respectively for **1, 2, 3** and **4**. From these experimental data, it is seen that the order of binding affinities of the complexes is in the order **4** > **3** > **2** > **1**, which is in agreement with the results observed from the electronic absorption and emission spectra. Furthermore, the observed quenching constants and binding constants of the cobalt(III) complexes suggest that the interaction of all the complexes with DNA should be of intercalation [34].

2.3.4. Viscosity studies

Optical photo physical titration generally provides necessary information, but not satisfactory evidence for the binding mode of the complexes with DNA. For further clarification of the binding mode, viscosity measurements need to be carried out on CT-DNA by varying the concentration of added complexes [35,36]. Fig. 7 shows the relative viscosity change of DNA in the presence of increasing amounts of complexes **1, 2, 3** and **4** respectively. These results suggest that the viscosity of DNA increases on addition of the cobalt(III) complexes. In general, the viscosity of DNA increases steadily when complexes intercalate between adjacent DNA base pairs. These experimental results indicate that complexes **1, 2, 3** and **4** bind to CT-DNA by the intercalation mode.

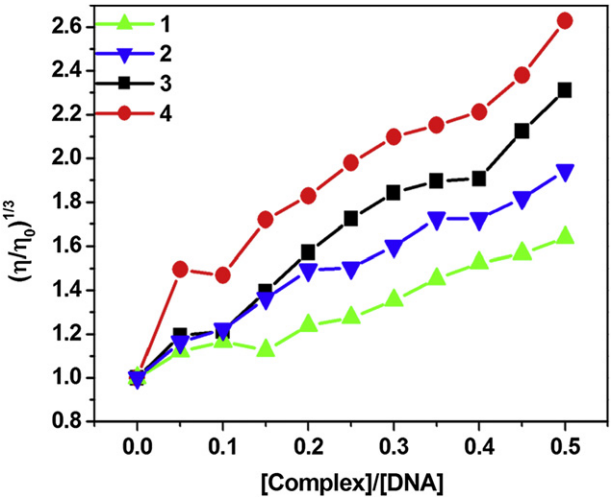

Fig. 7. Effect of increasing amount of the complexes (**1**–**4**) on the relative viscosity of CT-DNA at 25 °C.

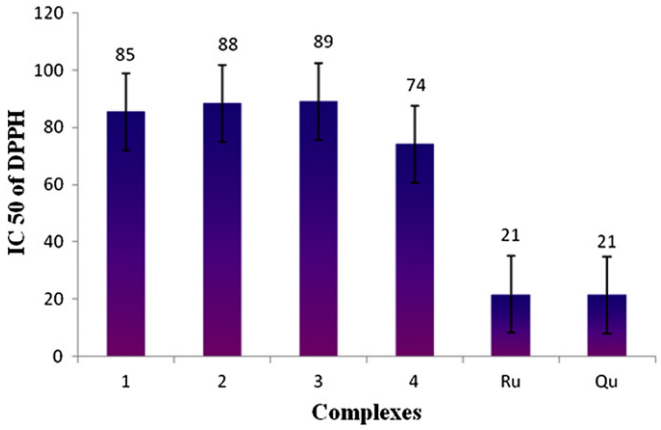

Fig. 8. 2-2′-diphenyl-1-picrylhydrazyl (DPPH) radical scavenging activity of the complexes (**1**–**4**) and the standards, Rutin (Ru) and Quercetin (Qu).

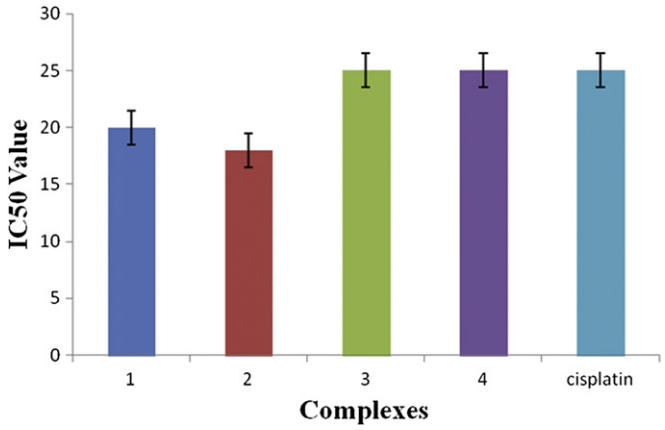

Fig. 9. Treatment of complexes that exert an antiproliferative effect on lung cancer cell line. A549 cells were treated with complexes (**1**–**4**) for 48 h. Control received appropriate carriers. Cell viability was assessed by MTT cell proliferation assay. Results shown are mean ± SD ($n = 9$) of the respective IC_{50} values, which are from three separate experiments performed in triplicate.

On the basis of absorption, emission, EB displacement and viscosity studies, we concluded that all the cobalt complexes can bind to CT-DNA in an intercalative mode and that the order of complexes binding to CT-DNA is **4** > **3** > **2** > **1**.

2.4. Antioxidant activity

Since the DNA binding experiments conducted so far revealed that the Co(III) complexes exhibit good DNA binding affinity, it is considered worthwhile to study the antioxidant activity of these compounds. 1,1-Diphenyl-2-picryl-hydrazyl (DPPH) assay is widely used for assessing the ability of radical scavenging activity and it is measured in terms of IC_{50} values. Because of the presence of odd electron, DPPH shows a strong absorption band at 517 nm in the visible spectrum. As this electron becomes paired off in the presence of a free radical scavenger, this absorption vanishes, and the resulting decolorization is stoichiometric with respect to the number of electrons taken up. The DPPH assay done for our complexes is shown in Fig. 8. It is seen from the results that the all the complexes exhibited moderate activities compared to the standards Rutin (Ru) and Quercetin (Qu). Statistically the scavenging effect of the compounds with DPPH radical is in the order **4** > **1** > **2** > **3.** The complex **4** showed better activity compared to the other three complexes, which may be due to the electron-withdrawing effect on terminal nitrogen atom of the ligands.

Ferric reducing antioxidant power (FRAP) is associated with the capacity to prevent peroxide formation, so that they can act as primary and secondary antioxidants. From the experimental data (Table 3) we suggest that the new Co(III) complexes exhibited strong reducing power. As expected, complexes **2** and **1** showed strong reducing power comparable with that of positive controls BHA and BHT. Since, our synthesised cobalt complexes are electron donors; they can terminate the oxidation chain reactions thereby reducing the oxidised intermediates into the stable form.

Table 3
Ferric Reducing Antioxidant Power (FRAP) of new Co(III) complexes.

Compound	FRAP (mM Fe (II) g^{-1})
1	2398.89 ± 277.82
2	4521.11 ± 38.92
3	1122.22 ± 93.95
4	1148.89 ± 48.34
BHA	1342.20 ± 157.20
BHT	7486.70 ± 162.30

2.5. Cytotoxic activity studies

2.5.1. MTT assay

The cytotoxicity assay for the new Co(III) complexes was assessed using the method of MTT reduction. Cisplatin was used as a positive control. All the complexes were found to be cytotoxic to lung cancer cell line (A549). The IC_{50} values (50% inhibition of cell growth for 48 h) for complexes **1**, **2**, **3** and **4** are 20 μM (**1**), 18 μM (**2**), 25 μM (**3**) and 25 μM (**4**) respectively (Fig. 9). The complexes exhibited higher cytotoxic effects on lung cancer cells with lower IC_{50} values indicating their efficiency in killing the cancer cells even at low concentrations. The cytotoxic effectiveness of these compounds with an IC_{50} of 20 μM (**1**) and 18 μM (**2**) were higher than that of cisplatin (25 μM). There are reports in the literature on the cytotoxic effects of the complexes with longer incubation time periods. The longer incubation period may result in the development of cellular resistance for that particular complex. Beckford et al have reported 50% inhibitory concentration of different complexes after an exposure for 72 h at μM concentrations. But, the data obtained for our complexes showed higher cytotoxicity with short incubation period (48 h). Hence, our data are highly significant when compared to the results of Beckford et al. [37]. Moreover, the IC_{50} values of our complexes are comparable with the reported IC_{50} values of standard anticancer drugs such as cisplatin.

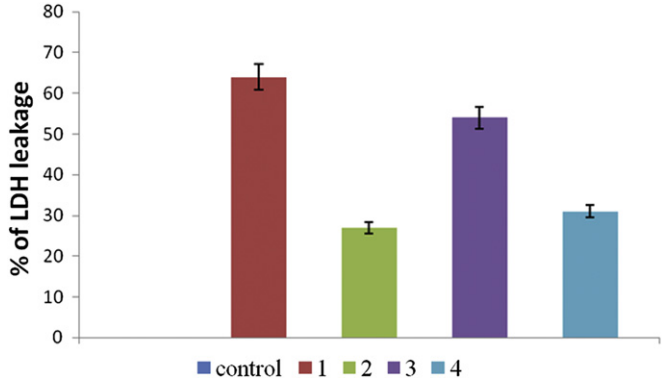

Fig. 10. Lactate dehydrogenase release by A549 cell line: Treatment with the complexes resulted in the release of LDH from the cell line. Results shown are mean ± SD ($n = 9$) of the percentage of LDH released, which are from three separate experiments performed in triplicate.

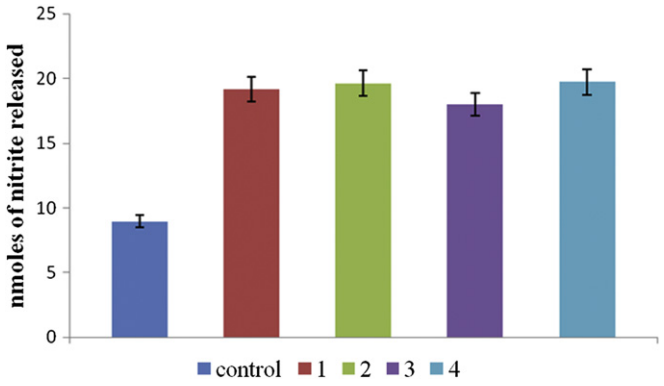

Fig. 11. Nitric oxide assay: treatment with the complexes resulted in the release of high levels of nitrite from both A549 cell line. Results shown are mean ± SD ($n = 9$) of the n moles of nitrite released, which are from three separate experiments performed in triplicate.

2.5.2. Lactate dehydrogenase release (LDH)

To further evaluate the toxicity, activity of LDH, a cytoplasmic enzyme released into surrounding media during cell death, was measured. Cell death by apoptosis leads to the release of cytoplasmic enzymes such as alkaline and acid phosphatase, glutamate-oxalacetate transaminase, glutamate pyruvate transaminase and arginosuccinatelyase. However, their use has been limited by the presence of low amount in many cells and hence an elaborate kinetic assay is required to measure the most enzyme activities. LDH is a stable cytoplasmic enzyme which is released into the culture medium following loss of membrane integrity resulting from apoptosis. LDH activity, therefore, can be used as an indicator of cell membrane integrity and serves as a general means to assess cytotoxicity resulting from chemical compounds or environmental toxic factors [38,39]. As can be seen from Fig. 10, a significant difference was observed between the control cells and cells treated with complexes **1**–**4** after 48 h of drug treatment. The four new Co(III) complexes lead to the release of significant level of lactate dehydrogenase by A549 cell line into the culture medium.

2.5.3. Nitric oxide assay

Nitric oxide (NO) has been assumed to have an important functional role in a variety of physiological systems. NO is derived from L-arginine by the action of NO synthase (NOS), an enzyme existing in three isoforms. Among them, two isoforms exist constitutively and the third isoform is an inducible form (iNOS) which is expressed in response to stress. NO is a gaseous signaling molecule, the stable product of which is nitrite. Nitric oxide is a well-known short-lived free radical produced non-enzymatically by iNOS which causes damage in most of the biomolecules, including DNA and protein [40]. The level of nitrite was found to increase significantly in complex treated cells compared to control (Fig. 11). The increased level of nitrite in the cell culture medium further confirms the cytotoxic effects of the presently studied complexes.

3. Conclusion

Four new 2-oxo-benzo[h]quinoline-3-carbaldehyde thiosemicarbazones ligands and their corresponding Co(III) complexes have been synthesized and characterized. The molecular structures of the complexes **2** and **3** have been determined by single crystal X-ray diffraction studies. The UV–visible, fluorescence spectroscopy and DNA solution viscosity measurements studies have revealed the ability of the complexes bind to DNA and supported the fact that the complexes bind to DNA via intercalation. The binding strength of the complexes with CT-DNA calculated with UV spectroscopic titrations have shown that the complex **4** has higher binding affinity to CT-DNA than the rest of the complexes. Ethidium bromide competitive binding studies have revealed that the facility of the complexes to displace EB from the EB-DNA complex. The antioxidant studies revealed that all the complexes exhibited moderate activities compared to the standards Rutin (Ru) and Quercetin (Qu). In addition, the *in vitro* cytotoxicity of complexes **1**–**4** against A549 cell line was assayed. The cytotoxicity of the complexes are affected by the various functional group attached to the terminal nitrogen atom, and the new Co(III) complexes showed considerable cytotoxic activity against A549 cell line. In our studies, we found that the antitumor property of the complexes was enhanced with the change in substitution at terminal nitrogen atom of the ligand.

4. Experimental section

4.1. Materials and instrumentation

All starting materials used throughout the experiments were of analytical or chemically pure grade. 2-Oxo-1,2-dihydrobenzo[h]quinoline-3-carbaldehyde and H_2L1-L4 were prepared according to the literature procedures [27,41]. Solvents were purified and dried according to standard procedures [42]. The reagents were purchased commercially and used without further purification unless otherwise noted. CT-DNA, Agarose and EB were obtained from Sigma–Aldrich and used as received. Elemental analyses (C, H, N, S) were performed on Vario EL III Elemental analyzer instrument. IR spectra (4000–400 cm^{-1}) for KBr disks were recorded on a Nicolet Avatar Model FT-IR spectrophotometer. ^1H NMR spectra were recorded on Bruker AMX 500 at 500 MHz. Melting points were determined with a Lab India instrument. Electronic absorption spectra were recorded using Jasco V-630 spectrophotometer. Emission spectra were measured with Jasco FP 6600 spectrofluorometer.

4.2. Preparation of the compounds

4.2.1. 2-Oxo-1,2-dihydrobenzo[h]quinoline-3-carbaldehyde thiosemicarbazone (H_2L1)

A methanolic solution of thiosemicarbazide (0.911 g, 0.01 mol) dissolved in warm methanol (50 mL) was added to a methanol solution (50 mL) containing 2-oxo-1,2-dihydro-benzo[h]quinoline-3-carbaldehyde (2.23 g, 0.01 mol). The mixture was refluxed for an hour during which period an yellow colour precipitate was formed. The reaction mixture was then cooled to room temperature and the solid compound was filtered. It was then washed with methanol and dried under vacuum. Yield: 87%. MP: 262–264 °C, Anal. calcd. for $C_{15}H_{12}N_4OS$ (%): C, 60.79; H, 4.08; N, 18.91; S, 10.82. Found (%): C, 60.93; H, 4.13; N, 18.86; S,10.77. IR (KBr, cm^{-1}): 3241(ms) ν(NH); 1643(s) ν(C=O); 1588, 1546(s) ν(C=N) + ν(C= C); 835(m) ν(C=S). UV–vis (DMSO), λ_{max} (nm): 274, 283, 373 (л → л*, n → л*). ^1H NMR (DMSO-D_6); δ 12.03 (s, N(1)H); δ 11.53 (s, N(3)H); δ 8.73 (s, 1H, C(3)H); δ 8.54(s, 1H, C(14)H); 8.23 (s, 2H, N(4)H); 7.21–8.15 (m, 6H, aromatic).

4.2.2. 2-Oxo-1,2-dihydrobenzo[h]quinoline-3-carbaldehyde N-methylthiosemicarbazone (H_2L2)

It was prepared using the same procedure as described for H_2L1 with 4-methyl-3-thiosemicarbazide (1.05 g, 0.01 mol) and 2-oxo-1,2-dihydrobenzo[h]quinoline-3-carbaldehyde (2.23 g, 0.01 mol). An yellow colour product was obtained. Yield: 85%. MP: 274–276 °C, Anal. calcd. for $C_{16}H_{14}N_4OS$ (%): C, 61.92; H, 4.55; N,

18.05; S, 10.33. Found (%): C, 61.87; H, 4.49; N, 18.09; S, 10.37. IR (KBr, cm^{-1}): 3317(ms) ν(NH); 1649(s) ν(C=O); 1550(s) ν(C=N) + ν(C=C); 811(m) ν(C=S). UV–vis (DMSO), λ_{max} (nm): 279, 373 (л → л*, n → л*). ^{1}H NMR (DMSO-D_6); δ 12.16 (s, N(1)H); δ 11.76 (s, N(3)H); δ 8.61 (s, 1H, C(3)H); δ 8.21(s, 1H, C(14)H); 8.15 (s, 1H, N(4)H); 7.67–7.98 (m, 6H, aromatic); 3.03 (s, 3H, C(17)H).

4.2.3. 2-Oxo-1,2-dihydrobenzo[h]quinoline-3-carbaldehyde N-ethylthiosemicarbazone (H_2L3)

It was prepared using the same procedure as described for H_2L1 with 4-ethyl- 3-thiosemicarbazide (1.19 g, 0.01 mol) and 2-oxo-1,2-dihydro-benzo[h]quinoline-3-carbaldehyde (2.23 g, 0.01 mol). An yellow colour product was obtained. Yield: 82%. MP: 259–260 °C, Anal. calcd. for $C_{17}H_{16}N_4OS$ (%): C, 62.94; H, 4.97; N, 17.27; S, 9.89. Found (%): C, 62.85; H, 4.87; N, 17.21; S, 9.78. IR (KBr, cm^{-1}): 3327(ms) ν(NH); 1648(s) ν(C=O); 1535(s) ν(C=N) + ν(C=C); 840(m) ν(C=S). UV–vis (DMSO), λ_{max} (nm): 295, 359 (л → л*, n → л*). ^{1}H NMR (DMSO-D_6); δ 12.43 (s, N(1)H); δ 11.67 (s, N(3)H); δ 8.91 (s, 1H, C(3)H); δ 8.81(s, 1H, C(14)H); 8.35 (s, 1H, N(4)H); 7.65–8.01 (m, 6H, aromatic); 3.34 (q, 2H, C(16)H); 1.21 (t, 3H, C(17)H).

4.2.4. 2-Oxo-1,2-dihydro-benzo[h]quinoline-3-carbaldehyde N-phenylthiosemicarbazone (H_2L4)

It was prepared using the same procedure as described for H_2L1 with 4-phenyl-3-thiosemicarbazide (1.67 g, 0.01 mol) and 2-oxo-1,2-dihydro-benzo[h]quinoline-3-carbaldehyde (2.23 g, 0.01 mol). An yellow colour product was obtained. Yield: 91%. MP: 245–246 °C, Anal. calcd. for $C_{21}H_{16}N_4OS$ (%): C, 67.72; H, 4.33; N, 15.04; S, 8.61. Found (%): C, 67.64; H, 4.47; N, 15.19; S, 8.58. IR (KBr, cm^{-1}): 3293(ms) ν(NH); 1652(s) ν(C=O); 1530(s) ν(C=N) + ν(C=C); 845(m) ν(C=S). UV–vis (DMSO), λ_{max} (nm): 279, 373, 392 (л → л*, n → л*). ^{1}H NMR (DMSO-D_6); δ 12.01 (s, N(1)H); δ 11.87 (s, N(3)H); δ 10.03 (s, 1H, C(3)H); δ 8.85(s, 1H, C(14)H); 8.39 (s, 1H, N(4)H); 7.35–7.98 (m, 11H, aromatic).

4.2.5. $[Co(HL1)_2]NO_3\cdot 4H_2O$ (**1**)

A warm methanolic solution (20 mL) containing H_2L1 (0.148 g, 0.05 mmol) was added to a methanolic solution (20 mL) of $Co(NO_3)_2\cdot 6H_2O$ (0.146 g, 0.05 mmol). The resulting red colour solution was refluxed for an hour. Dark red coloured crystalline powder was obtained on slow evaporation. They were filtered off, washed with cold methanol, and dried under vacuum. Yield: 83%. MP: 280–281 °C, Anal. calcd. for $C_{30}H_{30}CoN_9O_9S_2$ (%): C, 45.98; H, 3.86; N, 16.09; S, 8.18. Found (%): C, 45.83; H, 3.92; N, 16.01; S, 8.07. IR (KBr, cm^{-1}): 3293(ms) ν(NH); 1628(s) ν(C=O); 1482(s) ν(C=N); 754(m) ν(C–S). UV–visible (solvent MeOH, nm): 279 (ILCT); 431,455 (LMCT). ^{1}H NMR (DMSO-D_6); δ 13.94(s, N(1)H); δ 8.99 (s, 2H, N(4)H); δ 8.97(s, 1H, C(3)H); 8.86(s, 1H, C(14)H); 7.43–8.04 (m, 6H, aromatic).

4.2.6. $[Co(HL2)_2]NO_3\cdot 4H_2O$ (**2**)

It was prepared using the same procedure as described for **1** with H_2L2 (0.155 g, 0.05 mmol) and $Co(NO_3)_2\cdot 6H_2O$ (146 mg, 0.05 mmol). Dark red coloured crystals obtained were found to be suitable for X-ray diffraction. Yield: 79%. MP: 292–293 °C, Anal. calcd. for $C_{32}H_{34}CoN_9O_9S_2$ (%): C, 47.35; H, 4.22; N, 15.53; S, 7.91. Found (%): C, 47.49; H, 4.27; N, 15.62; S, 7.85. IR (KBr, cm^{-1}): 3359(ms) ν(NH); 1624(s) ν(C=O); 1511(s) ν(C=N); 729(m) ν(C–S).UV–visible (solvent MeOH, nm): 282 (ILCT); 433,456 (LMCT). ^{1}H NMR (DMSO-D_6); δ 13.92(s, N(1)H); δ 8.99(s, 1H, C(3)H); δ 8.97(s, 2H, N(4)H); 8.95(s, 1H, C(14)H); 7.62–8.04 (m, 6H, aromatic);

4.2.7. $[Co(HL3)_2]NO_3\cdot 4H_2O$ (**3**)

It was prepared using the same procedure as described for **1** with H_2L3 (0.162 g, 0.05 mmol) and $Co(NO_3)_2\cdot 6H_2O$ (146 mg, 0.05 mmol). Dark red coloured crystals obtained were found to be suitable for X-ray diffraction. Yield: 84%. MP: 286–288 °C, Anal. calcd. for $C_{34}H_{38}CoN_9O_9S_2$ (%): C, 48.62; H, 4.56; N, 15.02; S, 7.64. Found (%): C, 48.57; H, 4.61; N, 15.23; S, 7.68 IR (KBr, cm^{-1}): 3321(ms) ν(NH); 1625(s) ν(C=O); 1503(s) ν(C=N); 717(m) ν(C–S). UV–visible (solvent MeOH, nm): 278 (ILCT); 433,456 (LMCT). ^{1}H NMR (DMSO-D_6); δ 13.91(s, N(1)H); δ 8.98(s, 1H, C(3)H); δ 8.96(s, 2H, N(4)H); 8.95(s, 1H, C(14)H); 7.61–8.03 (m, 6H, aromatic); 3.37 (q, 2H, C(16)H); 1.15(t, 3H, C(17)H).

4.2.8. $[Co(HL4)_2]NO_3\cdot 4H_2O$ (**4**)

It was prepared using the same procedure as described for **1** with H_2L4 (186 mg, 0.05 mmol) and $Co(NO_3)_2\cdot 6H_2O$ (0.146 g, 0.05 mmol). Dark red coloured crystalline powder obtained. Yield: 89%. MP: 299–300 °C, Anal. calcd. for $C_{42}H_{38}CoN_9O_9S_2$ (%): C, 53.90; H, 4.09; N, 13.47; S, 6.85. Found (%):C, 53.82; H, 4.17; N, 13.36; S, 6.73. IR (KBr, cm^{-1}): 3255(ms) ν(NH); 1622(s) ν(C=O); 1490(s) ν(C=N); 745(m) ν(C–S). UV–visible (solvent MeOH, nm): 277 (ILCT); 441,463 (LMCT). ^{1}H NMR (DMSO-D_6); δ 13.7212.05 (s, 1H,N(1)H); 9.87 (s, 1H, N(4)H); 8.84 (s, 1H,C(1)H); 8.46 (s, 1H, C(6)H); 7.98–7.95 (m, 11H, aromatic).

4.3. Single-crystal X-ray diffraction studies

Single crystal X-ray diffraction data of **2** and **3** were collected at 100 K on an Oxford Xcalibur Eos (Mova) Diffractometer with X-ray generator operating at 50 kV and 1 mA, using Mo Kα radiation (λ = 0.7107 Å) [43]. The structures were solved and refined using SHELX97 module in the program suite WinGX [44,45]. The molecular diagrams were generated using ORTEP-3 and the packing diagrams were generated using Mercury 2.3. The geometric calculations were carried out by PARST95 and PLATON [46,47].

4.4. DNA binding studies

4.4.1. Titration experiments

All of the experiments involving the binding of compounds with CT-DNA were carried out in double distilled water with tris(hydroxymethyl)-aminomethane (Tris, 5 mM) and sodium chloride (50 mM) and adjusted to pH 7.2 with hydrochloric acid. A solution of CT-DNA in the buffer gave a ratio of UV absorbance of about 1.9 at 260 and 280 nm, indicating that the DNA was sufficiently free of protein. The DNA concentration per nucleotide was determined by absorption spectroscopy using the molar extinction coefficient value of 6600 M^{-1} cm^{-1} at 260 nm. The compounds were dissolved in a mixed solvent of 5% DMSO and 95% Tris–HCl buffer for all of the experiments. Absorption titration experiments were performed with a fixed concentration of the compounds (25 μM) while gradually increasing the concentration of DNA (5–25 μM). While measuring the absorption spectra, an equal amount of DNA was added to both the test solution and the reference solution to eliminate the absorbance of DNA itself. The same experimental procedure was followed for emission studies also. Further support for the complexes binding to DNA via intercalation is given through emission quenching experiments. DNA was pretreated with ethidium bromide for 30 min. Then the test solutions were added to this mixture of EB-DNA, and the change in the fluorescence intensity was measured. The excitation and the emission wavelength were 515 nm and 603–607 nm, respectively.

4.4.2. Viscosity measurements

Viscosity experiments were carried out using a Schott Gerate AVS 310 automated viscometer that was thermo stated at 25 °C in a constant temperature bath. The lengthening of the DNA helix has

been examined in the absence and presence of increasing amounts of complexes **1**–**4**. Flow time was measured with a digital stopwatch and for each sample the measurement was made in triplicates and the mean value of flow time was recorded. The obtained data are presented as $(\eta/\eta_0)^{1/3}$ versus the binding ratio r [48], where η is the viscosity of CT-DNA in the presence of complex, and η_0 is the viscosity of CT-DNA alone in buffer solution.

4.5. Antioxidant assays

4.5.1. 1,1-Diphenyl-2-picryl-hydrazyl (DPPH) assay

The DPPH radical scavenging activity of the complexes was measured according to the method of Blois [49]. The concentration of complexes necessary to decrease initial concentration of DPPH by 50% (IC_{50}) under the specified experimental condition was calculated. The test solution was incubated at 37 °C for 30 min in dark. The decrease in absorbance of DPPH was measured at 517 nm. The same experiment carried out without the test compounds served as control.

4.5.2. Ferric reducing antioxidant power (FRAP)

The antioxidant capacities of compounds and crude fractions were estimated according to the procedure described by Pulido et al. [50]. FRAP reagent (900 μL), prepared freshly and incubated at 37 °C, was mixed with 90 μL of distilled water and 30 μL of test sample or methanol (for the reagent blank). The test samples and reagent blank were incubated at 37 °C for 30 min in a water bath and the FRAP reagent contained 2.5 mL of 20 mmol/L TPTZ solution in 40 mmol/L HCl, 2.5 mL of 20 mmol/L $FeCl_3 \cdot 6H_2O$ and 25 mLof 0.3 mol/L acetate buffer (pH 3.6) were added at the end of incubation, the absorbance readings were taken immediately at 593 nm using a spectrophotometer. Methanolic solutions of known Fe (II) concentration, ranging from 100 to 2000 μmol/L, ($FeSO_4.7H_2O$) were used for the preparation of the calibration curve. The parameter Equivalent Concentration (EC_1) is defined as the concentration of antioxidant having a ferric-TPTZ reducing ability equivalent to that of 1 mmol/L $FeSO_4 \cdot 7H_2O$. EC_1 was calculated as the concentration of antioxidant giving an absorbance increase in the FRAP assay equivalent to the theoretical absorbance value of a 1 mmol/L concentration of Fe(II) solution, determined using the corresponding regression equation.

4.6. Cytotoxicity assays

4.6.1. 3-(4,5-Dimethylthiazol-2-yl)- 2,5- diphenyltetrazolium bromide (MTT) assay

Cytotoxic effect of the four new complexes on human lung cancer cells (A549) were assayed by the 3-(4,5-dimethylthiazol-2-yl)- 2,5- diphenyltetrazolium bromide (MTT) assay [51]. The cells were seeded at a density of 10,000 cells per well, in 200 μl and then the samples **1**, **2, 3** and **4** were added to the cells at a final concentration of 1, 10, 25 and 50 μM in the cell culture media. After 48 h, the wells were treated with 20 μl MTT (5 mg/mL PBS) and incubated at 37 °C for 4 h. The purple formazan crystals formed were dissolved in 200 μL DMSO and read at 570 nm in a micro plate reader.

4.6.2. Release of lactate dehydrogenase (LDH)

LDH activity was determined by the linear region of a pyruvate standard graph using regression analysis and expressed as percentage leakage as described previously [52]. Briefly, to a set of tubes, 1 cm^3 of buffered substrate (lithium lactate) and 0.1 cm^3 of the media or cell extract were added and tubes were incubated at 37 °C for 30 min. After adding 0.2 cm^3 of NAD solution, the incubation was continued for another 30 min. The reaction was then arrested by adding 0.1 cm^3 of DNPH reagent and the tubes were incubated for further period of 15 min at 37 °C. After this 0.1 cm^3 of media or cell extract was added to blank tubes after arresting the reaction with DNPH. Then 3.5 cm^3 of 0.4 N sodium hydroxide was added to all the tubes. The colour developed was measured at 420 nm with a UV–visible spectrophotometer. The amount of LDH released was expressed in percentage.

4.6.3. Nitric oxide (NO) assay

The amount of nitrite was determined by the literature method [53]. Nitrite reacts with Griess Reagent to give a coloured complex measured at 540 nm. To 100 μL of the medium, 50 μL of Griess reagent I was added, mixed and allowed to react for 10 min. This was followed by the addition of 50 μL of Griess reagent II and the reaction mixture was mixed well and incubated for another 10 min at room temperature. The pink colour developed was measured at 540 nm in a microquant plate reader (Biotek Instruments).

Acknowledgments

Council of Scientific and Industrial Research, New Delhi, India [Grant No. 01(2216)/08/EMR-II & 21(0745)/09/EMR-II] for the financial assistance received, and the University Grants Commission, New Delhi, for the award of a Fellowship in Science for Meritorious Students (RFSMS) to E. R under the UGC-SAP-DRS programme, are gratefully acknowledged.

Appendix. Supplementary material

Crystallographic data for the structures reported in this paper have been deposited with the Cambridge Crystallographic Data Centre (CCDC) as supplementary publication number CCDC-861100, and CCDC-861101 for complexes **2**, and **3** respectively. Copies of the data can be obtained free of charge from the CCDC (12 Union Road, CambridgeCB2 1EZ, UK; Tel.: +44 1223 336408; Fax: +44 1223 336003; e-mail: deposit@ccdc.cam.ac.uk; Web site http://www.ccdc.cam.ac.uk).

References

[1] T. Boulikas, M. Vougiouka, Oncol. Rep. 10 (2003) 1663–1682.
[2] E. Wong, C.M. Giandomenico, Chem. Rev. 99 (1999) 2451–2466.
[3] M. Galanski, V.B. Arion, M.A. Jakupec, B.K. Keppler, Curr. Pharm. Des 9 (2003) 2078–2089.
[4] D. Wang, S. Lippard, J. Nat. Rev. Drug Discov. 4 (2005) 307–320.
[5] P.V. Bernhardt, G.A. Lawrance, in: J.A. McCleverty, T.J. Meyer (Eds.), Comprehensive Coordination Chemistry II, vol. 6, 2003, pp. 1–45 (Chapter 1).
[6] E. Vinuelas-Zahinos, F. Luna-Giles, P. Torres-Garcia, M.C. Fernandez-Calderon, Eur. J. Med. Chem. 46 (2011) 150–159.
[7] M.B. Ferrari, F. Bisceglie, C. Casoli, S. Durot, I.M. Badarau, G. Pelosi, E. Pilotti, S. Pinelli, P. Tarasconi, J. Med. Chem. 48 (2005) 1671–1675.
[8] M.B. Ferrari, F. Bisceglie, G. Pelosi, P. Tarasconi, R. Albertini, A. Bonati, P. Lunghi, S. Pinelli, J. Inorg. Biochem. 83 (2001) 169–179.
[9] D.X. West, M.A. Lockwood, Trans. Met. Chem. 22 (1997) 447–452.
[10] B. Peng, H. Chao, B. Sun, F. Gao, L.N. Ji, J. Zhang, Trans. Met. Chem. 32 (2007) 271–277.
[11] P. Nordell, P. Lincoln, J. Am. Chem. Soc. 127 (2005) 9670–9671.
[12] P. Barraja, P. Diana, A. Montalbano, G. Dattolo, G. Cirrincione, G. Viola, D. Vedaldi, F.D. Acqua, Bioorg. Med. Chem. 14 (2006) 8712–8728.
[13] J.T. Kuethe, A. Wong, C.X. Qu, J. Smithtrovich, I.W. Davies, D.L. Hughes, J. Org. Chem. 70 (2005) 2555–2567.
[14] J. DeRuiter, A.N. Brubaker, W.L. Whitmer, J.L. Stein, J. Med. Chem. 29 (1986) 2024–2028.
[15] P. Hewawasam, W. Fan, J. Knipe, S.L. Moon, C.G. Boissard, V.K. Gribkoff, J.E. Starztt, Bioorg. Med. Chem. Lett. 12 (2002) 1779–1783.
[16] D.S. Raja, N.S.P. Bhuvanesh, K. Natarajan, Eur. J. Med. Chem. 46 (2011) 4584–4594.
[17] D.S. Raja, N.S.P. Bhuvanesh, K. Natarajan, Inorg. Chem. 50 (2011) 12852–12866.
[18] R. Prabhakaran, P. Kalaivani, R. Jayakumar, M. Zeller, A.D. Hunter, S.V. Renukadevi, E. Ramachandran, K. Natarajan, Metallomics 3 (2011) 42–48.

[19] E. Ramachandran, P. Kalaivani, R. Prabhakaran, N.P. Rath, S. Brinda, P. Poornima, V.V. Padma, K. Natarajan, Metallomics 4 (2012) 218–227.
[20] E. Ramachandran, P. Kalaivani, R. Prabhakaran, M. Zeller, J.H. Bartlett, P.O. Adero, T.R. Wagner, K. Natarajan, Inorg. Chim. Acta (2011). doi:10.1016/j.ica.2011.12.045.
[21] D.S. Raja, G. Paramaguru, N.S.P. Bhuvanesh, J.H. Reibenspies, R. Renganathan, K. Natarajan, Dalton Trans. 40 (2011) 4548–4559.
[22] P. Kalaivani, R. Prabhakaran, F. Dallemer, P. Poornima, E. Vaishnavi, E. Ramachandran, V. Vijaya Padma, R. Renganathan, K. Natarajan, Metallomics 4 (2012) 101–113.
[23] P.F. Rapheal, E. Manoj, M.R.P. Kurup, E. Suresh, Polyhedron 26 (2007) 607–616.
[24] M.C. Rodriguez-Arguelles, E.C. Lopez-Silva, J. Sanmartin, A. Bacchi, C. Pelizzi, F. Zani, Inorg. Chim. Acta 357 (2004) 2543–2552.
[25] A.F. Tanious, D.Y. Ding, D.A. Patrick, C. Bailly, R.R. Tidwell, W.D. Wilson, Biochemistry 39 (2002) 12091–12101.
[26] C.Y. Zhong, J. Zhao, Y.B. Wu, C.X. Yin, P. Yang, J. Inorg. Biochem. 101 (2007) 10–18.
[27] Z.-C. Liu, B.-D. Wang, Z.-Y. Yang, Y. Li, D.D. Qin, T.-R. Li, Eur. J. Med. Chem. 44 (2009) 4477–4484.
[28] Z.-C. Liu, B.-D. Wang, B. Li, Q. Wang, Z.-Y. Yang, T.-R. Li, Y. Li, Eur. J. Med. Chem. 45 (2010) 5353–5361.
[29] A. Wolf, G.H. Shimer, T. Meehan, Biochemistry 26 (1987) 6392–6396.
[30] D.S. Raja, N.S.P. Bhuvanesh, K. Natarajan, Eur. J. Med. Chem. 47 (2012) 73–85.
[31] F.J. Meyer-Almes, D. Porschke, Biochemistry 32 (1993) 4246–4253.
[32] G.M. Howe, K.C. Wu, W.R. Bauer, Biochemistry 19 (1976) 339–347.
[33] Y.B. Zeng, N. Yang, W.S. Liu, N. Tang, J. Inorg. Biochem. 97 (2003) 258–264.
[34] R. Senthil Kumar, S. Arunachalam, V.S. Periasamy, C.P. Preethy, A. Riyasdeen, M.A. Akbarsh, J. Inorg. Biochem. 103 (2009) 117–127.
[35] S. Satyanarayana, J.C. Dabroviak, J.B. Chaires, Biochemistry 31 (1992) 9319–9342.
[36] D. Lawrence, V.G. Vaidyanathan, B.U. Nair, J. Inorg. Biochem. 100 (2006) 1244–1251.
[37] F.A. Beckford, M. Shaloski, G. Leblanc, J. Thessing, L.C.L. Alleyne, A.A. Holder, L. Li, N.P. Seeram, Dalton Trans. (2009) 10757–10764.
[38] E. Bonfoco, D. Krainc, M. Ankarcrona, P. Nicotera, S.A. Lipton, Proc. Natl. Acad. Sci. 92 (1995) 7162–7166.
[39] C. Legrand, J.M. Bour, C. Jacob, J. Capiaumont, A. Martial, A. Marc, M. Wudtke, G. Kretzmer, C. Demangel, D. Duval, J. Hache, J. Biotechnol. 25 (1992) 231–243.
[40] L. Yu, P.E. Gengaro, M. Niederberger, T.J. Burke, R.W. Schriert, Proc. Natl. Acad. Sci. 91 (1994) 1691–1695.
[41] M.K. Singh, A. Chandra, B. Singh, R.M. Singh, Tetrahedron Lett. 48 (2007) 5987–5990.
[42] A.I. Vogel, Text Book of Practical Organic Chemistry, fifth ed. Longman, London, 1989, p. 268.
[43] Oxford Diffraction, CrysAlis PRO CCD and CrysAlis PRO RED, Oxford Diffraction Ltd, Yarnton, England, 2009.
[44] G.M. Sheldrick, Acta Crystallogr. Sect. A 64 (2008) 112–122.
[45] L.J. Farrugia, J. Appl. Crystallogr. 32 (1999) 837–838.
[46] L.J. Farrugia, J. Appl. Crystallogr. 30 (1997) 565.
[47] A.L. Spek, J. Appl. Crystallogr. 36 (2003) 7–13.
[48] G. Cohen, H. Eisenberg, Biopolymers 8 (1969) 45–55.
[49] M.S. Blois, Nature 181 (1958) 1199–1200.
[50] R. Pulido, L. Bravo, F. Sauro-Calixto, J. Agric. Food Chem. 48 (2000) 3396–3402.
[51] T. Mossman, J. Immunol. Methods 65 (1983) 55–63.
[52] W.E.C. Wacker, D.D. Ulmer, B.L. Valee, New Eng. J. Med. 255 (1956) 449–455.
[53] D.J. Stueher, M.A. Marletta, J. Immunol. 139 (1987) 518–525.